NASA CONTRACTOR REPORT

NASA CR-729

NASA CR-7

OPTICAL RADAR MEASUREMENTS OF THE ATMOSPHERE

by J. D. Lawrence, Jr., F. R. Crownfield, Jr., and M. P. McCormick

Prepared by
COLLEGE OF WILLIAM AND MARY
Williamsburg, Va.
for Langley Research Center

NATIONAL AERONAUTICS AND SPACE ADMINISTRATION • WASHINGTON, D. C. • APRIL 1967

OPTICAL RADAR MEASUREMENTS OF THE ATMOSPHERE

By J. D. Lawrence, Jr., F. R. Crownfield, Jr.,
and M. P. McCormick

Distribution of this report is provided in the interest of
information exchange.   Responsibility for the contents
resides in the author or organization that prepared it.

NATIONAL AERONAUTICS AND SPACE ADMINISTRATION

TABLE OF CONTENTS

I. INTRODUCTION

An accurate description of the molecular and particulate content of the earth's atmosphere and their diurnal, seasonal and altitude variation is necessary in order to derive an atmospheric model. Direct measurements may be made up to about 30 km by balloon-borne instruments, and above 150 km satellite experiments provide useful data. The region 30-150 km, however, remains accessible only to indirect measurements or rocket probes.

Indirect light scattering methods have necessarily dominated investigations of this region. The searchlight probe technique was first attempted by Synge[1] in 1930, and a number of subsequent search-light investigations of the atmosphere have been carried out.[2-9] Volz and Goody[10] have carried out extensive investigations of the particulate content of the atmosphere by measurement of twilight scattering. Newkirk and Eddy[11] have made skylight measurements up to 25 km using a balloon-borne coronagraph, and from these measurements have calculated the particle size and vertical distribution of stratospheric aerosols. Direct measurement of stratospheric aerosols has been made by Junge and Manson.[12]

The development of the giant pulse laser provides a monochromatic light source of very high intensity which may be used in an optical radar system to investigate the molecular and particulate content of the atmosphere. Using this technique, Fiocco and Smullin[13] have reported optical echoes from heights up to about 140 km, which have tentatively been interpreted in terms of meteoric fragmentation. Fiocco and Grams[14] have reported observing an aerosol layer at approximately 20 km. Observations of the

stratospheric aerosol have also been made by Collis and Ligda[15] and Collis, Fernald and Ligda.[16]

The present report will discuss several aspects of optical radar investigations of the atmosphere currently under way at The College of William and Mary. Theoretical considerations will be presented which allow estimates of the optical radar returns from various altitudes, and these will be used to discuss signal-to-noise ratios and to optimize various system parameters. Following this, the experimental equipment will be described, and finally some sample data will be presented and discussed.

II. THEORETICAL CONSIDERATIONS

The atmosphere will be considered a mixture of aerosols describable by Mie Theory, and molecules describable by Rayleigh Theory. If an electromagnetic flux F is incident on a volume ΔV, the power scattered into a detector which subtends a solid angle Ω is given by

$$P_{detector} = F \, q \, (\sigma_R + \sigma_{Mie}) \, \Delta V \, \Omega, \tag{1}$$

where $\sigma_R + \sigma_{Mie}$ is the scattering cross-section per unit volume, assumed to include both Rayleigh scatter (σ_R) and Mie scatter (σ_{Mie}). q is the attenuation of the signal (total extinction) in propagating from the scatterer to the detector. In general the cross-sections σ_R and σ_{Mie} depend on the angle between the incident propagation direction and the scattered propagation direction, and on the polarization state of the incident radiation. The scattering volume is given by

$$\Delta V = \frac{\pi}{4} (z\delta_T)^2 \, \Delta L, \tag{2}$$

where

z = height of scattering volume

δ_T = beam divergence angle of laser

ΔL = pulse length (determined by half-power points).

The solid angle subtended by the detector is

$$\Omega = \frac{A_r}{z^2} , \tag{3}$$

where A_r is the area of the receiver.

The incident flux is given by

$$F = q \; \frac{\bar{P}}{\frac{\pi}{4} (z\delta_T)^2} \; , \tag{4}$$

where $\bar{P}$ is the average power delivered by the laser.

Substituting equations (2), (3), and (4) into equation (1), we obtain

$$P_{det} = \frac{\bar{P} \; \Delta L \; q^2 A_r}{z^2} (\sigma_R + \sigma_{Mie}). \tag{5}$$

IIa. Rayleigh Scattering

The absolute Rayleigh cross-section for backscatter is

$$\sigma_R = k^4 \alpha^2 \; N(z) \; f, \tag{6}$$

where

$$k = \frac{2\pi}{\lambda} = \text{wave number of incident radiation}$$

$$\alpha = \text{polarizability}$$

$$N(z) = \text{number density,}$$

and

$$f = \frac{3 \; (2 + \Delta)}{6 - 7\Delta} \; ,$$

where Δ is the depolarization factor. For atmospheric air, G.
de Vaucouleurs[17] has found

$$\Delta = 0.031.$$

Thus

$$f = 1.054.$$

The polarizability of sea level air for incident radiation in the

visible is given as

$$\alpha = 1.73 \times 10^{-30}.$$

This value may be assumed valid at all altitudes of interest in the present
work.

Therefore

$$\sigma_R = 2.087 \times 10^{-32} \; N(z)$$

Then the power incident on the detector due to Rayleigh

4

scattering is

$$P_{R \text{ det}} = 2.087 \times 10^{-32} \frac{\bar{P} \, \Delta L \, q^2 \, A_r \, N(z)}{z^2}, \tag{7}$$

where

$$\Delta L = \frac{c\tau}{2} \, ,$$

since the light will be received simultaneously from $\frac{c\tau}{2}$, i.e., only half the scattering volume contributes to the instantaneous backscatter. τ is the pulse width measured at half power points.

For the 60-inch diameter mirror ($A_r = 1.823 \ m^2$), optical efficiency 0.5, used in our system we obtain

$$P_{R \text{ det}} = 2.851 \times 10^{-24} \frac{\bar{P}\tau q^2 N(z)}{z^2} \, .$$

Assuming the laser energy output is 1 joule

$$\bar{P} = 1 \text{ joule}/\tau.$$

Then

$$P_{R \text{ det}} = 2.851 \times 10^{-24} \frac{q^2 \, N(z)}{z^2} \, .$$

This gives the power incident on the detector. The photomultiplier used is an RCA 7265 whose cathode radiant sensitivity at 6943 Å is 0.014 amp/watt. The gain is given as 9.35×10^6. Assuming an optical efficiency of 0.7 for the filters, the detected anode current is

$$i_{R \text{ det}} = 2.612 \times 10^{-19} \frac{q^2 \, N(z)}{z^2} \, . \tag{8}$$

Using the values of number density from the U. S. Standard Atmosphere 1962 and the extinction values from L. Elterman,[18] for 0.7μ, the photocurrent for various heights due to molecular scattering has been computed and is listed in Table I.

Table I

$z(km)$	$N(m^{-3})$	$\dfrac{N}{z^2}(m^{-5})$	q^2	$\dfrac{q^2 N}{z^2}\,(m^{-5})$	$i_R\ det$ (amperes)	$V = i_R 50\Omega$
5	1.53×10^{25}	6.12×10^{17}	0.687	4.20×10^{17}	1.10×10^{-1}	5.50 v
10	8.60×10^{24}	8.60×10^{16}	0.669	5.75×10^{16}	1.50×10^{-2}	0.750 v
15	4.05×10^{24}	1.80×10^{16}	0.664	1.20×10^{16}	3.13×10^{-3}	0.157 v
20	1.85×10^{24}	4.63×10^{15}	0.658	3.05×10^{15}	7.96×10^{-4}	39.8 mv
25	8.34×10^{23}	1.33×10^{15}	0.655	8.71×10^{14}	2.27×10^{-4}	11.4 mv
30	3.83×10^{23}	4.26×10^{14}	0.651	2.77×10^{14}	7.23×10^{-5}	3.62 mv
35	1.76×10^{23}	1.44×10^{14}	0.650	9.36×10^{13}	2.44×10^{-5}	1.22 mv
40	8.31×10^{22}	5.19×10^{13}	0.648	3.36×10^{13}	8.77×10^{-6}	0.439 mv
45	4.09×10^{22}	2.02×10^{13}	0.648	1.31×10^{13}	3.42×10^{-6}	0.171 mv
50	2.14×10^{22}	8.56×10^{12}	0.648	5.55×10^{12}	1.45×10^{-6}	0.0725 mv

IIb. Scattering by Large Particles

Any investigation of the scattering properties of the atmosphere must take into consideration the contribution of large particles. Assuming that the particulate matter present in the atmosphere may be considered a collection of spherical particles of index of refraction η, the absolute cross-section for back scatter is given by

$$\sigma_{Mie} = \frac{1}{k^2} \sum_r i\,(\alpha,\ \eta,\ 180^{\circ})\ N_{Mie}\,(r), \tag{9}$$

where

$i\,(\alpha,\ \eta,\ 180^{\circ})$ = the Mie intensity function for 180°, scattering

$N_{Mie}\,(r)$ = the number density of particles of radius r,

and

$$\alpha = \frac{2\pi r}{\lambda} = \text{particle size parameter.}$$

It can be seen that, even under the assumption that the particles are spherical, the scattering properties of each particle must be known in order to determine σ_{Mie}. It should be noted that atmospheric particles are of finite size; in consequence, asymptotic approximations of the intensity functions do not provide sufficient accuracy.

The size distribution function of stratospheric aerosols has been measured directly by Junge and his collaborators.[12] The Junge law for stratospheric aerosols is given by

$$\frac{d\,n\,(r)}{d\,\log\,r} = c\,r^{-\nu}, \tag{10}$$

where $\frac{d\,n\,(r)}{d\,r}$ is the particle concentration and c is a parameter dependent on the total number of particles.

The cross-section for backscatter then becomes

$$\sigma_{Mie} = \int_{r_1}^{r_2} \frac{1}{k^2} i\,(\alpha, \eta, 180^\circ)\, d\,n\,(r).$$

The intensity functions for $\eta = 1.5$, which represents an average value for stratospheric aerosols, have been calculated by a number of investigators. For example, R. Giese[19] has tabulated these functions for $\eta = 1.5$ and size parameters given by 0.2 (0.1) 159.

A Fortran II computer program has been written to compute the intensity functions for arbitrary index and scattering angle in order to fit our data to a number of atmospheric models. The intensity functions for $\eta = 1.5$ and size parameters .05 (.01) 2, and 2 (.1) 50 for backscatter are given in the Appendix. As computer time becomes available these computations will be extended to larger values of α.

The complete integral

$$\int_{r_1}^{r_2} \frac{r^2}{\alpha^2} \frac{i_1 + i_2}{2}\, d\,n\,(r),$$

has been tabulated by Bullrich[20] for a number of parameters representative of the atmospheric aerosol distribution. Also of interest is the size distribution function proposed by Deirmendjian[21] to describe the aerosol size distribution of natural water clouds and atmospheric haze. This function has been successfully used by a number of investigators to fit atmospheric aerosol scattering measurements. Computer programs are currently being developed to evaluate these integrals for various distribution functions using the exact Mie Theory for i.

A number of experimental determinations of the parameters contained in the size distribution function has been made using light scattering techniques. Penndorf[22] has examined the vertical distribution of large particles in the troposphere. He concludes that the number of Mie particles

8

decrease exponentially up to 4 or 5 km and above that altitude the number density remains constant. The size distribution was observed by Junge and his collaborators[12] to remain invariant up to about 25 km; the number density showed a broad maximum between 15 and 23 km with little seasonal variation. Newkirk and Eddy[11] using a balloon-borne coronagraph have measured the aerosol concentration to about 25 km. Their measurements indicate a change in particle size distribution with an apparent concentration of the smaller Mie particles in a layer at an altitude of about 20 km. The existence of this "dust" layer has been demonstrated by the direct measurements of Junge and his collaborators[12], by the twilight studies of Volz and Goody[10] and by the rocket measurements of Rossler and Vassy.[23] Initially, we shall perform calculations using some of these data as summarized in the A. F. C. R. L. "Clear Standard Atmosphere" of Elterman.[18]

The optical radar method, used by Fiocco and his collaborators[13], shows promise as a technique for studying scattering layers in the mesosphere and lower thermosphere. The existence of an aerosol layer at about 80 km has long been suspected. Mikirov[24] has estimated the extinction due to large particles in this region to be about five times the Rayleigh value. This layer has been observed by Fiocco and his collaborators[13]. Other experimenters [25], [26] have attempted to observe the 80 km dust layer but echoes as intense as those observed by Fiocco have not been detected. Noctilucent clouds also occur in the region 80-90 km and measurements of their altitude and drift are fundamental to understanding atmospheric dynamical processes. In addition, Fiocco and Colombo[27] have found evidence of a scattering layer in the region 110-140 km which they have tentatively interpreted in terms of meteoric fragmentation.

The problem of interpretation of optical radar data has been reviewed by Deirmendjian[28]. Among many processes which can produce enhancement of the return signal are: changes in size distribution and particle concentration, changes in index of refraction associated with photochemical processes, and turbulence. It is of course impossible to separate these processes by measurements at one wavelength, and for this reason measurements at harmonic wavelengths of ruby and neodymium are planned. It should be noted, however, that harmonic generation is a relatively inefficient process; consequently, measurements of dust at very high altitudes will be difficult. Furthermore, since only three wavelengths will be available, it will be possible to determine only three parameters at any given height. It therefore seems desirable to attempt to fit a model with two parameters as a function of height; if the results are not consistent, the model can be rejected.

Initially a Junge distribution will be tried, varying the parameters so that exinction coefficients in agreement with the A. F. C. R. L. "Clear Standard Atmosphere" can be obtained; the resulting model will be used to calculate Mie scattering return which can be compared with experiment.

III. NOISE CONSIDERATIONS

Noise in the system originates from the signal, background, photomultiplier, and load resistor. This includes   shot noise associated with signal, background, and photomultiplier dark current given by

$$i_N = u \ (2ei \wedge f)^{\frac{1}{2}} = u[2e \ (i_D + i_S + i_B) \wedge f]^{\frac{1}{2}}, \qquad (12)$$

where i_D = dark current of the photomultiplier at the photocathode

i_S = signal current at the photocathode

i_B = background current at the photocathode

μ = gain of the photomultiplier

e = electron charge

$\wedge f$ = passband of the measuring instrument

[The randomness of the secondary emission at the dynodes adds additional noise equivalent to multiplying equation (12) by a factor of 1.2 [29]]and the Johnson (thermal) noise associated with the load resistor, given by

$$i_{JN} = \frac{(4kTR \Delta f)^{\frac{1}{2}}}{R} \ , \qquad (13)$$

where k = Boltzman's constant

T = absolute temperature

R = value of the load resistor.

The thermal noise contribution is negligible compared to shot noise as can be seen by comparing Equation (12) and Equation (13). Any signal current greater than 10^{-18} amperes (6 electrons/sec) makes the shot noise greater than the Johnson noise for a load resistor of 100 Ω.

Ignoring the Johnson noise and the randomness of the secondary emission, the signal-to-noise ratio is given by

$$S_N = u\frac{i_S}{i_{N'}} = \frac{i_S}{[2e\Delta f(i_S+i_B+i_D)]^{\frac{1}{2}}},$$ (14)

S_N can be increased by increasing i_S, decreasing Δf, or decreasing $(i_B + i_D)$. The system may be optimized by the correct choice of these parameters. Solving Equation (14) for i_S,

$$i_S = (e\Delta f)S_N^2 + [(e\Delta f)^2 S_N^4 + 2(e\Delta f)S_N^2(i_B+i_D)]^{\frac{1}{2}}.$$ (15)

We shall accept $S_N = (10)^{\frac{1}{2}}$ as a minimum S_N for signal detection. A plot of i_S versus Δf for $S_N = (10)^{\frac{1}{2}}$, and $(i_B+i_D) = 0$, 10^{-14}, and 10^{-11} amperes is given in Figure 1. These values represent the extreme cases of no dark current or background, maximum dark current and no background, and maximum dark current and maximum background. The minimum resolution $\frac{c\tau}{2}$ corresponding to each bandwidth is given on the top margin, and the maximum height corresponding to the calculated current expected for Rayleigh scattering is given on the right margin. Several important conclusions can be made by examining these curves.

(1) For $\Delta f \geq 10^8$ cps, the limiting factor is the shot noise produced by the signal. Reducing the background and dark current to zero will not allow a smaller signal to be detected.

(2) Decreasing the bandwidth to 10^5 cps and reducing the background level below that of the dark current will allow heights of up to 45 km to be investigated. Lowering the dark current will not allow a smaller signal to be detected.

(3) Lowering the bandwidth below 10^4 cps would destroy the height resolution of the system.

To compute the sky background noise, the average sky background power P_B incident on the receiver must be calculated:

MINIMUM   RESOLUTION,   Kilometers

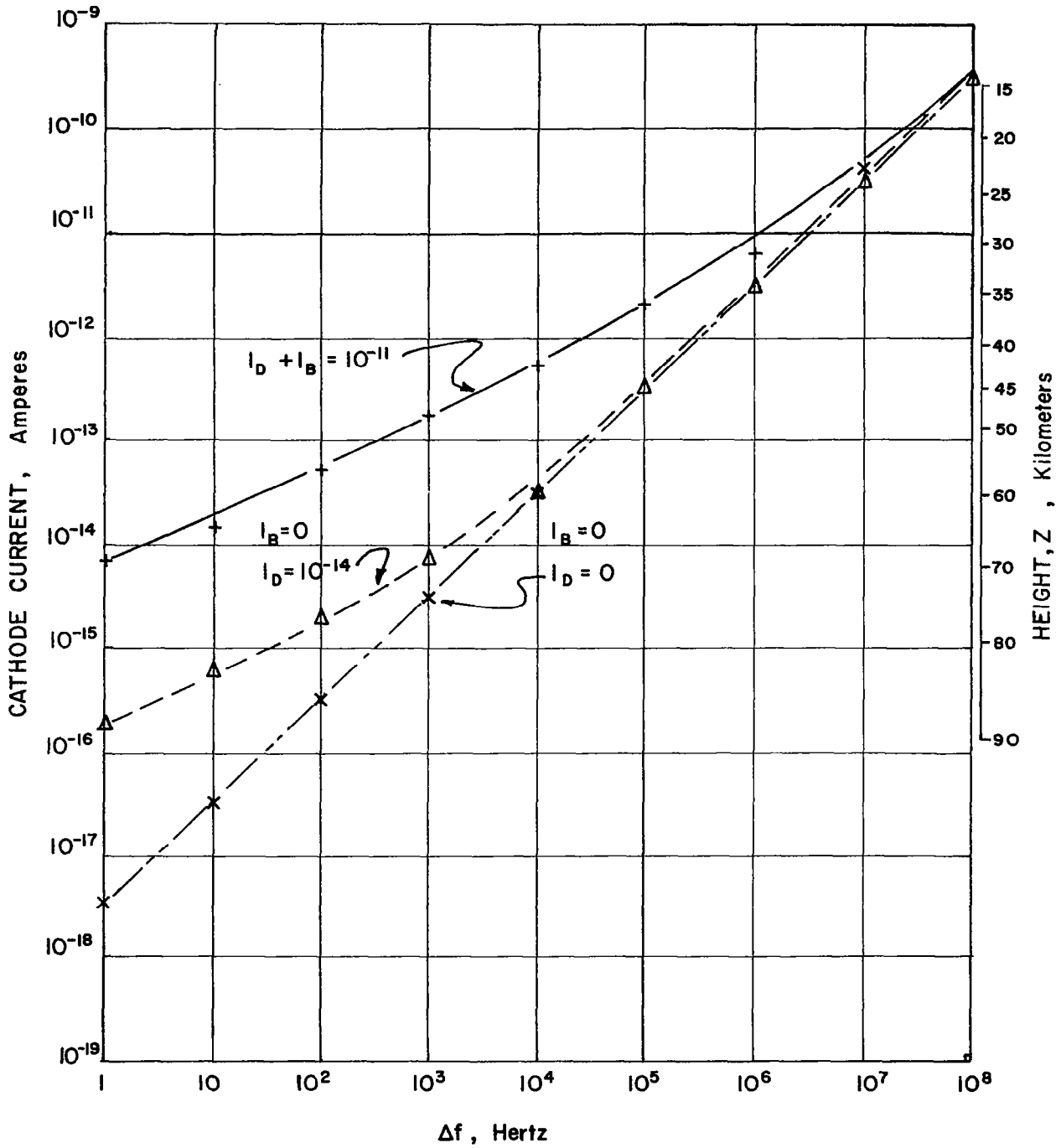150,000   15,000   1,500   150   15   1.5   0.15   0.015   0.0015

CATHODE CURRENT , Amperes

10^{-9}
10^{-10}
10^{-11}
10^{-12}
10^{-13}
10^{-14}
10^{-15}
10^{-16}
10^{-17}
10^{-18}
10^{-19}

$I_D + I_B = 10^{-11}$

$I_B = 0$
$I_D = 10^{-14}$

$I_B = 0$
$I_D = 0$

HEIGHT, Z , Kilometers

15
20
25
30
35
40
45
50
60
70
80
90

1   10 10^2 10^3 10^4 10^5 10^6 10^7 10^8

Δf , Hertz

Figure I

13

$$P_B = \Omega \, A_R \, q_R \, \Delta\lambda \, R_\lambda, \tag{16}$$

where R_λ is the background radiance in watts/m^2/steradian/Å; Ω is the solid angle of the receiver in steradians; $\Delta\lambda$ is the passband of the filter and S-20 photocathode response; q_R is the efficiency of the receiving optics, and A_R is the receiver area in m^2. R_λ is given by Ketay[30] for the day sky to be 2×10^{-3} watts/m^2/steradian/Å for the 7000 Å region. Pavlova[31] gives a value of 2×10^{-9} watt/m^2/steradian/Å for the nighttime air glow in the region of 7000 Å. These values agree with the electrometer measurements of the background radiation incident on our system.

As seen in Equation (16), this background power may be minimized by limiting the receiver's field of view to that of the transmitter's field of view and/or reducing the passband of the filter system. $\Delta\lambda$ may be reduced by using a very narrow band interference filter chosen so that the highest signal-to-noise ratio is achieved. When using such a filter, the incident light must be rendered parallel to within $\pm 3^{\circ}$. The angle of divergence of the transmitter may be decreased by using a collimator in front of the laser. The angular demagnification is given by

$$D_T = \frac{f_r}{f_e},$$

where f_r is the focal length of the entrance lens and f_e is the focal length of the exit lens. The angle of divergence of the transmitter is given by

$$\delta_T = \frac{f_r}{f_e} \, \delta_L,$$

where δ_L is the angular divergence of the laser. Thus shot noise due to the background can be decreased by decreasing the angular divergence of the receiver, decreasing $\Delta\lambda$, and increasing the angular demagnification of the collimator.

Another source of background is the fluorescence associated with the laser transmission. The wavelength of this radiation is the same as the giant pulse, and therefore, cannot be discriminated against with the use of filters. The amplitude of the fluorescence is much smaller than the laser pulse but persists for about 2 milliseconds. Scattering of this fluorescence radiation from the lower atmosphere is comparable to the laser pulse scattering from very high altitudes. For this reason, a rotating shutter has been designed and is currently being assembled to eliminate this source of background.

The maximum height which can be investigated increases as the bandwidth of the receiving system is decreased. The use of an electronic bandwidth much less than 10^4 cps, however, destroys the height resolution of the system. Thus a different measurement technique must be used if altitudes much above 50 km are to be investigated.

For measuring the return from high altitudes, it will be necessary to use a photon counting system. With such a system, the number of pulses produced by the emission of photoelectrons will be counted and stored in a digital delay line. In the nth "channel" will be stored those pulses occurring during an interval of length ℓ and at a time t_n after the laser emission; t_n being different for each channel. Thus the number of counts in each channel represents the return from a height interval $\Delta h = \frac{c\ell}{2}$ about a height $h = \frac{ct_n}{2}$. The advantage of this system is that the signal-to-noise ratio can be improved with no loss of resolution by taking the total number of counts in each channel produced by a number of successive shots.

The number of counts in any time interval obeys a Poisson distribution; therefore, the standard deviation is $\sqrt{\bar{c}t}$ where $\bar{c}$ is the mean number of counts per unit time during the interval and t is the total counting time.

Thus the signal to fluctuation ratio is

$$S = \frac{t C_s}{[t(C_s + C_D + C_B)]^{\frac{1}{2}}},$$ (17)

where C_s, C_D, and C_B are the number of counts per unit time due to signal, dark current, and background, respectively, and t is the total counting time. It is seen that $S \rightarrow t^{\frac{1}{2}}$, so that increasing t increases S. If the system is fired N times and the number of counts in one channel are collected for an interval $\mathcal{l}$ for each shot, then the total counting time is t = N$\mathcal{l}$, while the resolution is $\frac{c\mathcal{l}}{2}$. Thus increasing N increases S with no change in the resolution of the system.

Let us now consider the minimum signal that can be detected with such a system. Solving for C_s, we get

$$C_s = \frac{S^2}{2t} \{1 + [1 + \frac{4t}{S^2}(C_D + C_B)]^{\frac{1}{2}}\}.$$ (18)

If we chose $S^2 = 10$ (in analogy with the discussion given for Equation (15) and Figure 1), we get the minimum counting rate which can be detected with a given counting time.

$$C_s = \frac{5}{t} \{1 + [1 + \frac{2t}{5}(C_D + C_B)]^{\frac{1}{2}}\}$$ (19)

A plot of C_s vs t for values of $(C_D + C_B) = 0$, 0.6×10^5/sec, and 0.6×10^8/sec [corresponding to values of $(i_D + i_B) = 0$, 10^{-14} amp, and 10^{-11} amp] is given in Figure 2. From this curve, it is possible to determine the approximate height from which return from molecular scatter can be measured, using the calculated values of the Rayleigh scattering return signal. Figure 2 shows that if an ideal system with background and dark current equal to zero is assumed, a counting time of 10^{-5} sec would allow a counting rate of 10^6 counts/sec to be measured. This corresponds to a return from approximately 49 km. If 10 successive shots with $\mathcal{l}=10^{-5}$sec are taken, then t=10^{-4}sec and
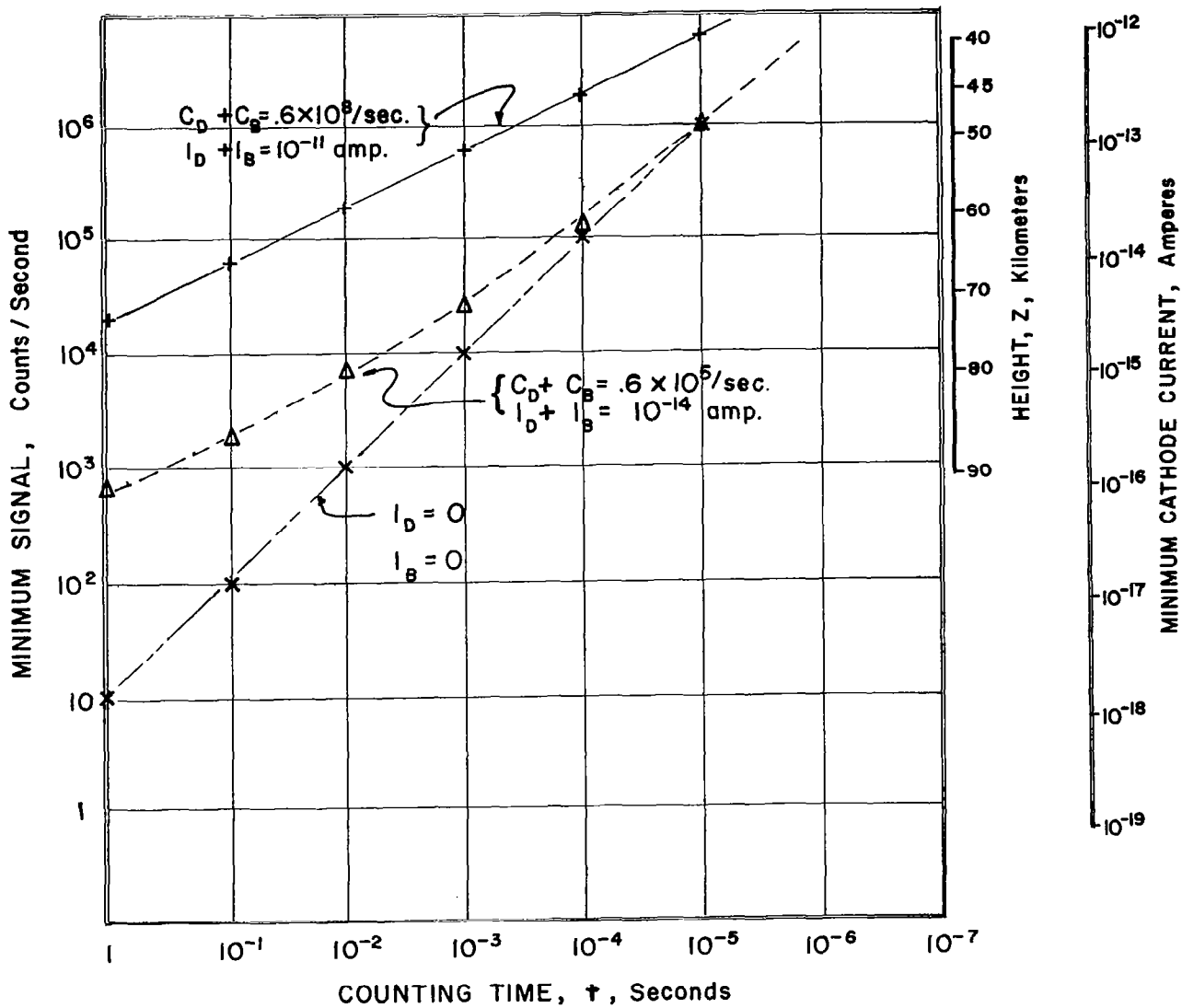
Figure 2

17

the maximum height from which return can be measured is approximately 63 km, while the resolution remains at 1.5 km. Similarly, if 10 shots with $t=10^{-4}$ sec (15 km resolution) are taken, then return from 77 km can be measured. Greater altitudes can be reached by taking a larger number of shots.

It is apparent from the curve that if return from above 50 km is to be measured, then not only should the background be made as low as possible, but also that it will be beneficial to reduce the dark current of the P. M. tube. For example, if $t=10^{-3}$ sec, the reduction of the dark current from its normal 0.6×10^{5} photoelectrons/sec to less than 10^{3} photoelectrons/sec will increase the maximum height by about 7 km, with greater reductions in height possible for longer counting times. Note, however, that the background must be lower than the dark current if the effect is to be this large. By cooling the P. M. tube, it is possible to reduce the dark current to the order of 200 photoelectrons per second, which makes this source of noise in these experiments negligible.

IV. EQUIPMENT

General

The basic experimental arrangement is shown in Figure 3. The laser pulse is monitored with a set of beam splitters whose axes are separated by 90° allowing a portion of the beam to fall on a diffuse white screen which lies in the field of view of a photodiode. The beam splitters' orientation provides polarization insensitivity. The output of the photodiode is displayed on a Tektronix 585 oscilloscope and provides a measure of the laser pulse width. The charge through the photodiode gives a number proportional to the total number of emitted photons and the total light energy. This charge is stored in a capacitor and the resulting voltage measured by an electrometer giving an energy readout to within $\pm$ 10%. The focus electrode of the photomultiplier detector is biased 30 v negative with respect to the cathode thereby defocusing the tube. A monostable multivibrator (see Figure 4) is triggered by a delayed pulse synchronous with the emission of the giant laser pulse. The monostable multivibrator produces a positive gate with a rise time of about 1 u sec and a variable width and height. This gate is applied to the focusing electrode thereby focusing the detector for a length of time determined by the gate width. The anode of the photomultiplier is direct coupled to a variable gain operational amplifier used to limit the frequency passband of the system. This output is direct coupled to an amplifier with logarithmic response over three decades and displayed, simultaneously with the gating waveform, on a dual beam oscilloscope. Figure 5 shows the triggering sequence as it evolves in time.
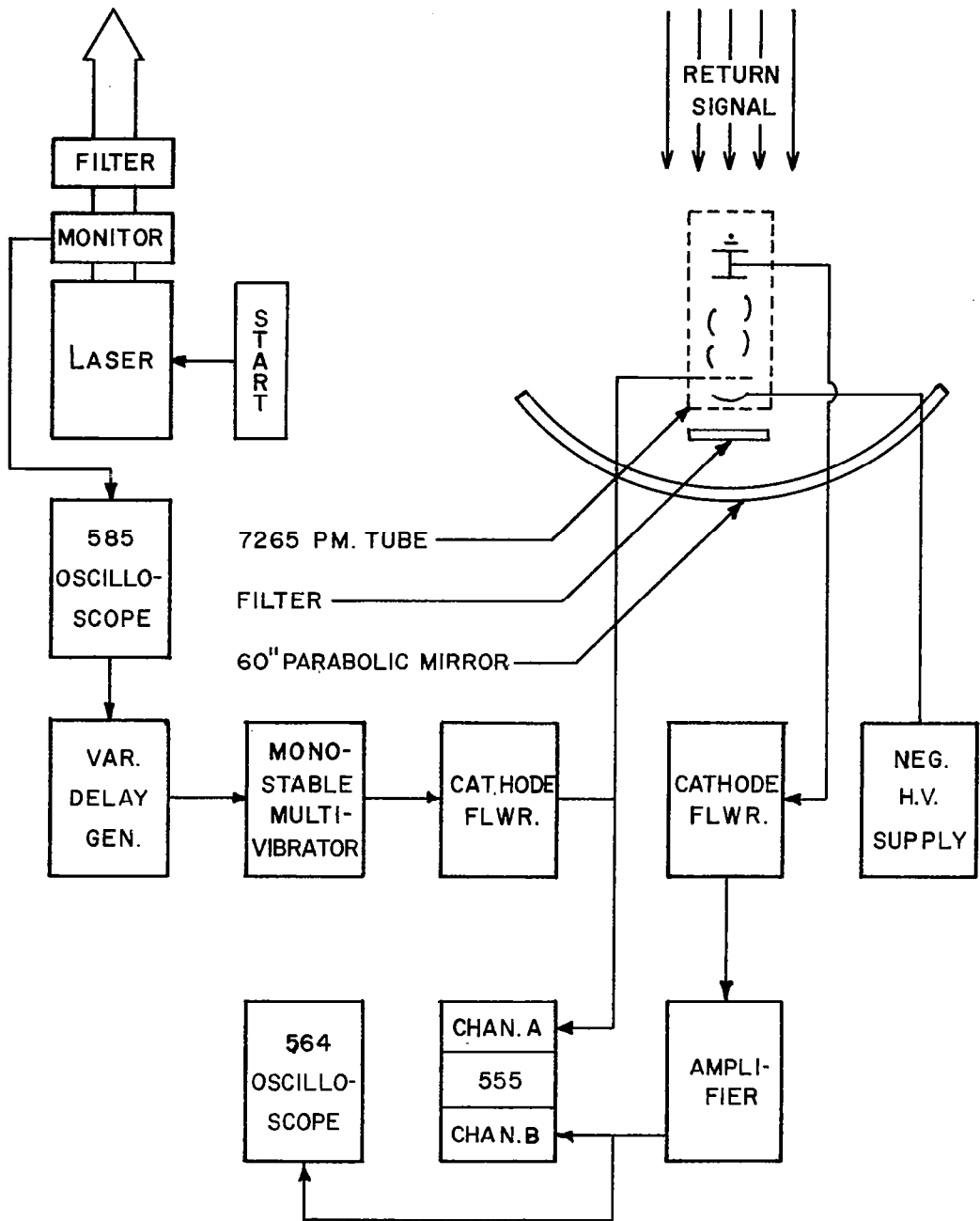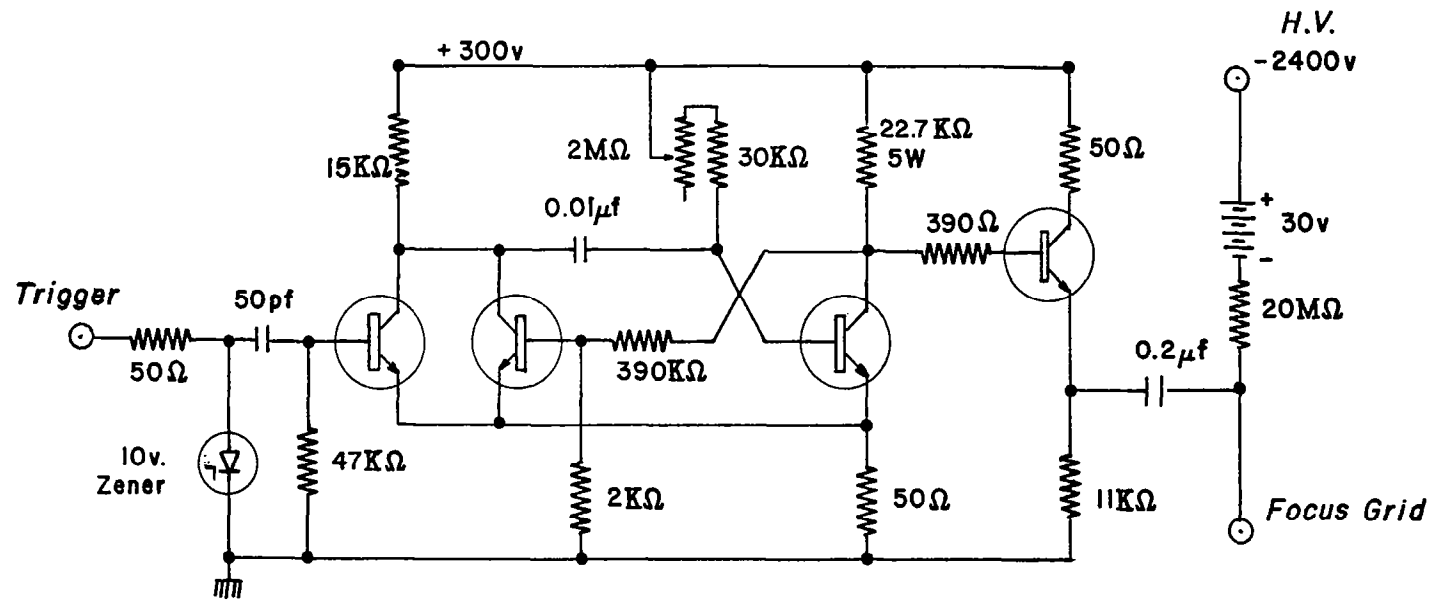
RETURN
SIGNAL

FILTER

MONITOR

LASER

START

585
OSCILLO-
SCOPE

7265 PM. TUBE

FILTER

60" PARABOLIC MIRROR

VAR.
DELAY
GEN.

MONO-
STABLE
MULTI-
VIBRATOR

CATHODE
FLWR.

CATHODE
FLWR.

NEG.
H.V.
SUPPLY

564
OSCILLO-
SCOPE

CHAN. A

555

CHAN. B

AMPLI-
FIER

Figure 3

H.V.
−2400 v

+ 300v

15KΩ

2MΩ 30KΩ

0.01μf

22.7 KΩ
5W

50Ω

390 Ω

+ 30v
−

20MΩ

Trigger

50pf

50Ω

10v.
Zener

47KΩ

390KΩ

2KΩ

50Ω

11KΩ

0.2μf

Focus Grid

All Transistors – TRS 3504

MONOSTABLE
MULTIVIBRATOR

Figure 4

TRIGGER   SEQUENCE

INITIAL TRIGGER FROM LASER MONITOR	TIME ⟶
585 GATE	
VARIABLE DELAY GENERATOR PULSE	
MONOSTABLE MULTIVIBRATOR GATE, VARIABLE HEIGHT & WIDTH	
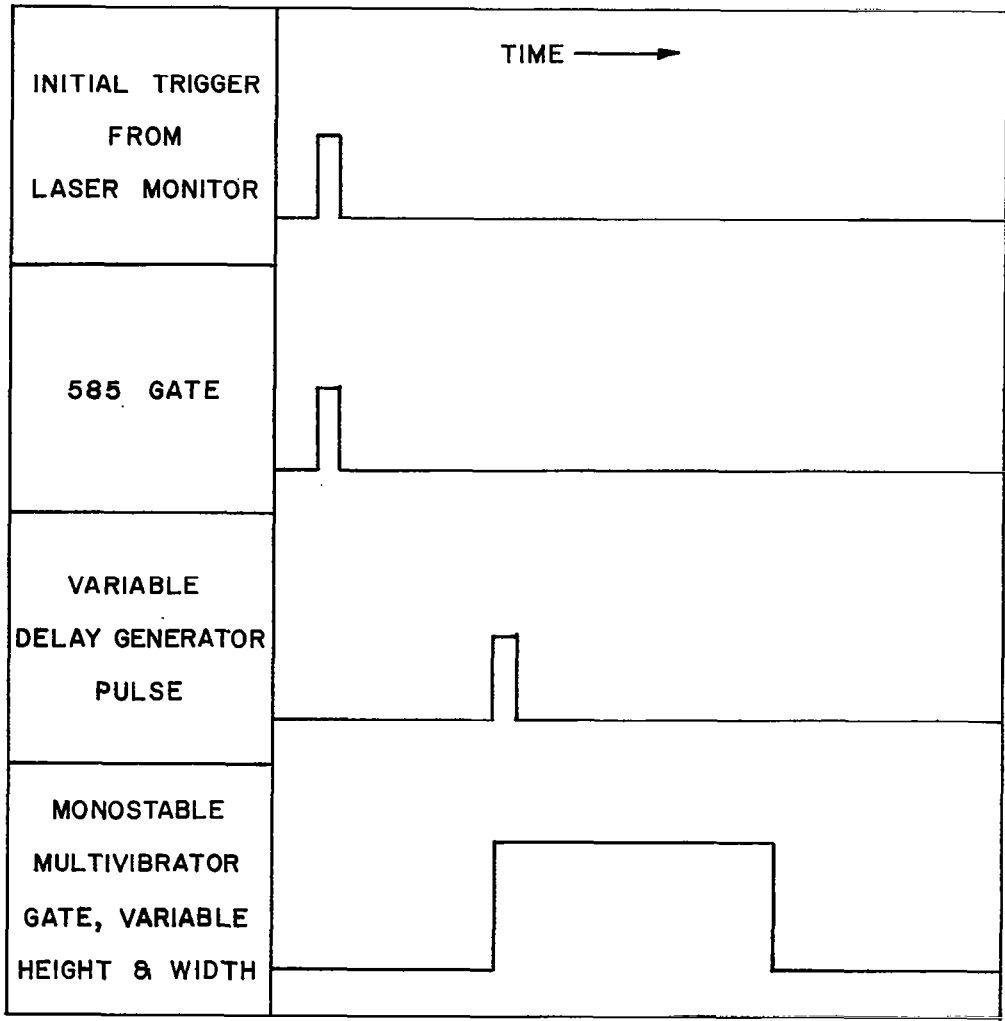
Figure 5

IVa. Receiver System

The receiver system consists of a sixty inch searchlight mirror (focal length = 25.54 inches) in a steerable mount. The photomultiplier detector is positioned behind the focal plane on a precision mount with 5 degrees of freedom. An iris is used to limit the field of view of the mirror to a calculated value of about 8 milliradians. In order to limit the night-sky background, a Wratten No. 70 filter is positioned in front of the photomultiplier. This filter has a sharp cutoff at 6500 Å; and, when used in conjunction with a photomultiplier having an S-20 photocathode spectral response, gives a bandpass of about 700 Å. Several methods of incorporating a narrow band interference filter into this system have been studied. A wide angle plastic doublet lens with an index of 1.49 and a transmittance of 75% was studied with a ray trace program and calculated to collimate the radiation from 50% of the mirror surface to within ± 3 degrees which would permit the use of a 20 Å interference filter. In view of the quality of the searchlight mirror surface, it is difficult to attach a great deal of significance to such calculations, although the method does show some promise of improving our signal to noise ratio.

Very recently a 12 inch Cassegrain telescope system has been made available for these studies and will permit backscatter measurements to be carried out with very narrow band interference filters.

IVb. Transmitter System

Two lasers have been incorporated into the system in order to provide measurements at two wavelengths nearly simultaneously. One of these laser systems can be operated with a $4"x\frac{9}{16}"$ ruby rod or a $6"x\frac{3}{8}"$ neodymium rod. The ruby rod is Q-switched with a cryptocyanine-methanol solution giving an energy output of about 2 joules; the neodymium rod is Q-switched

with Kodak 9740 dye-chlorobenzene solution and yields an energy output of
about 0.8 joule. The second laser system contains a .7"x$\frac{1}{2}$" Brewster angle
ruby rod which is Q-switched by uranyl glass and has an energy output of
about 2 joules. These laser systems when used in conjunction with a
frequency doubling cell of potassium dihydrogen phosphate give us the
capability of operating at three usable wavelengths: 0.53 μ, 0.6943 μ, and
0.3472 μ. The neodymium fundamental at 1.06 μ will be of little use because
of the lack of a suitable photodetector for this wavelength. Each laser
is enclosed in a light tight container with a monitor and collimator
positioned at the output. The collimator enables a reduction of the
receiver field of view by reducing the beam divergence by a factor of five.
The collimator consists of negative and positive quartz lenses arranged so
that the focal point of the first (negative) lens coincides with the focal
point of the second lens. Both laser systems are temperature controlled in
order to prevent detuning into a water vapor absorption line.

To assist in the alignment of the receiver and transmitter, a
telescope has been aligned with the axis of the laser. The back beam of
a gas laser is directed into the ruby or neodymium laser cavity and the
reflected beam is made coincident with it. The output beam of the gas
laser will therefore indicate the direction of the giant pulse. This
beam is aligned with a telescope mounted on the laser table and once this
alignment is completed, the telescope is used to align the laser with the
receiver axis. This is accomplished by positioning the image of the moon
on the focal point of the mirror while simultaneously viewing the moon
through the telescope. Final alignment is accomplished by adjusting the
axis of the laser for maximum return.

Soon to be incorporated in the transmitting system is a high speed

rotating shutter. A 400 cycle hysteresis synchronous motor will be used to rotate a balanced aluminum disk at 24,000 rpm. A magnetic pickup positioned near the disk will provide a pulse to trigger the laser. This pulse will be delayed so that the shutter opening will align itself with the laser exit port when the laser Q-switches. The shutter is open for 75 μ sec and closes in 78 μ sec; therefore, no fluorescence can enter the receiver after 153 μ sec (23 km). Below this height the scattered laser pulse signal is much greater than the scattered fluorescence.

V. EXPERIMENTAL RESULTS

After the laser is fired, the return signal is measured as a function
of time by a photomultiplier whose output can be displayed with both
logarithmic and linear amplification on a dual beam oscilloscope. If
desired, the gating waveform may replace one of these output signals. No
attempt has been made at this point in the experiments to count photons.
The bandwidth of the receiving system is limited by a variable gain operational
amplifier and the optical efficiency may be reduced by neutral density
filters.

Typical results are plotted in Figure 6, where $\Delta f = 10^6$ cps and a
number two neutral density filter was used. Each data set represents the
return from a single laser transmission normalized at 15 km to the value
predicted for molecular scatter from the U. S. Standard Atmosphere (1962).
Figure 1 indicates that for $\Delta f = 10^6$ cps measurements can be made to
about 28-35 km. These values are realized experimentally as shown in Figure 6.
Returns from higher altitudes ($\approx$ 40 km) have been measured, but drift in the
d. c. level of the logarithmic amplifier makes them uncertain. Most of
our measurements show an enhancement in the scattering profile near 20 km
in agreement with the results of other investigators[14],[25], and the
return above 30 km shows close agreement with Rayleigh Theory.

A number of interesting meteorological phenomena in the lower atmosphere
are evident in many records. Figure 7 is an example of this. The top trace
is a logarithmic display of the return while the bottom trace is a low
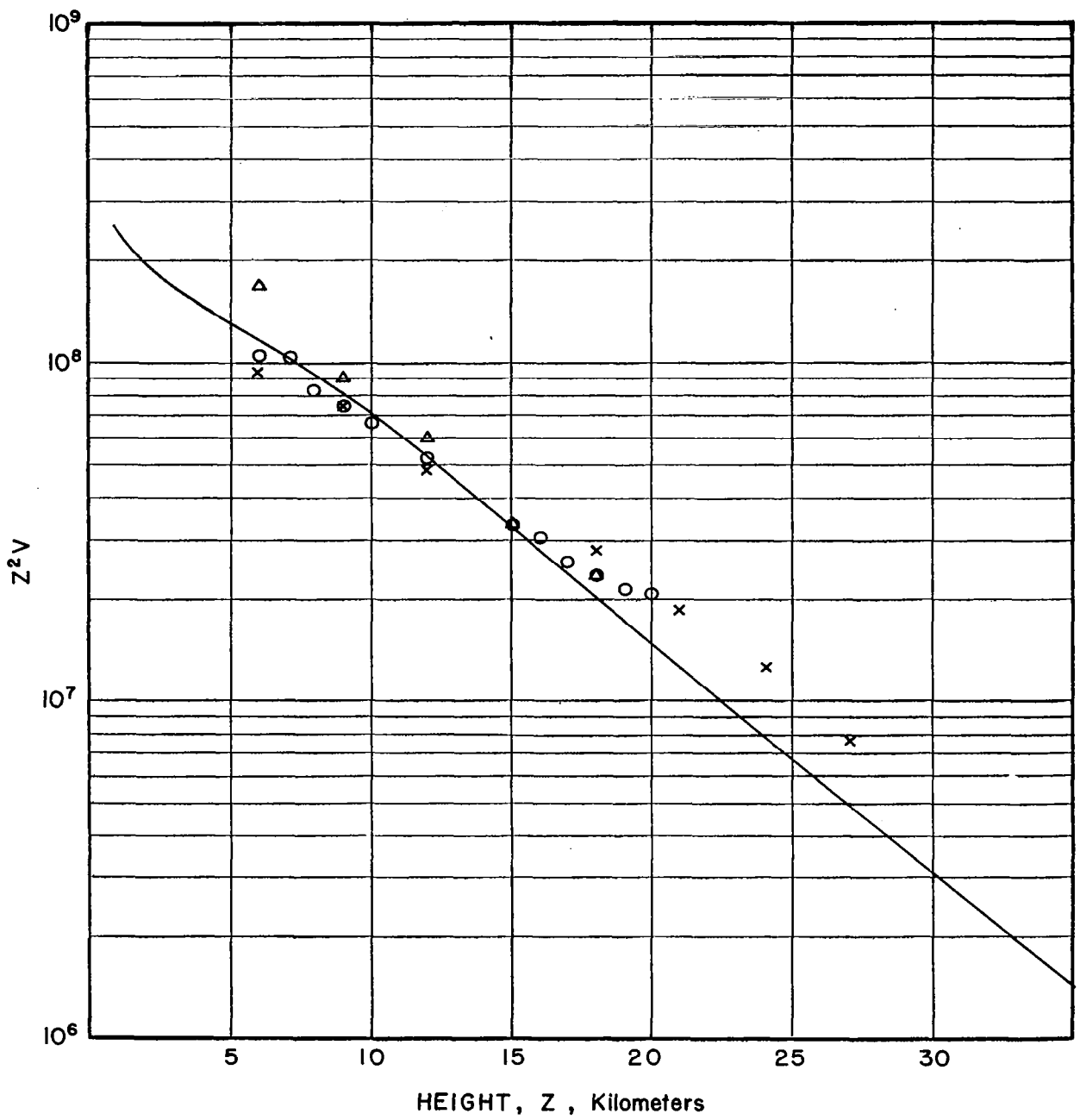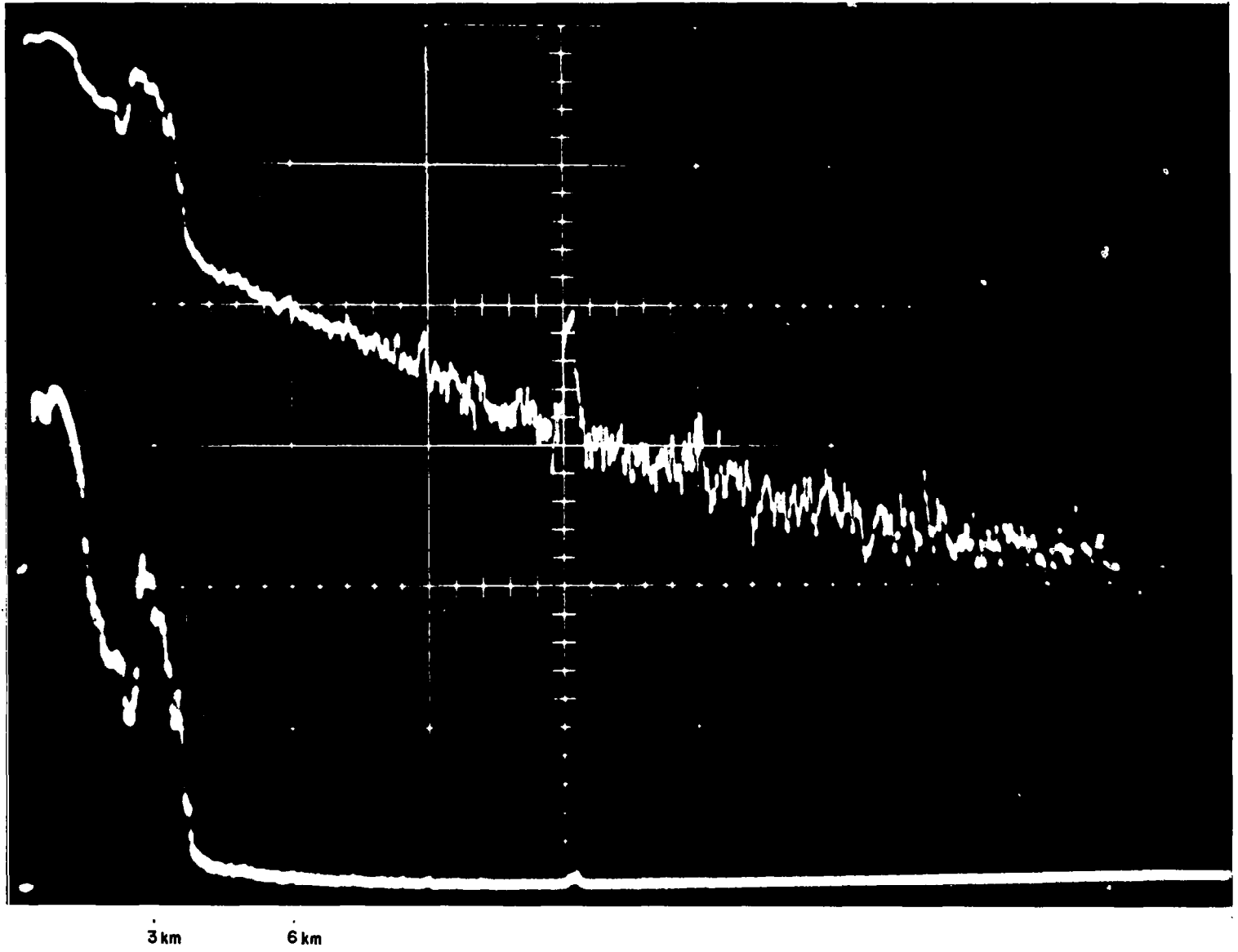sensitivity linear display. The enhancement evident at 12 km is a factor

Figure 6

27

Figure 7

3 km   6 km

20μsec/div.

28

of 10 greater than the clear air return from this height. The echo is probably produced by a cirrus cloud. In addition, this record shows an aerosol structure centered at 3 km which is probably an altocumulus cloud. A region of high return is also evident in Figure 8 at about 10.5 km. The shape of the return is typical of many records obtained. If the region of high aerosol concentration represents a cirrus cloud, a qualitative explanation of the structure of the return can be given: the values of the single particle intensity function for a given index of refraction show large fluctuations as a function of particle radius. The particles in the extremities of a cloud may have sizes which tend to scatter the incident radiation more effectively. Alternatively, cirrus clouds might be made up of ice needles oriented so that scatter or attenuation would be stronger in various parts of the cloud. Finally, different size crystal aggregates would change the scattering properties within a given cloud.

Shown in Figures 9a and 9b is an example of the three-dimensional mapping of the aerosol structure which can be made with optical radar. Figure 9a shows the return for 90° elevation while Figure 9b shows the return for an elevation angle of 31° recorded one minute later. These records were made about thirty minutes before the passage of a cold front, and indicate an aerosol concentration near 2.0 km. The record made at the lower elevation angle indicates that the effect is real since at lower elevation angles the peak moves out in time and broadens.

An example of the repeatability of the results is given in Figure 10. In this case the laser was made to multi-pulse and return from two laser transmissions are shown. Three enhancements appearing at 10 μ sec, 33 μ sec, and 46 μ sec after the laser pulse are shown. Each laser trans-
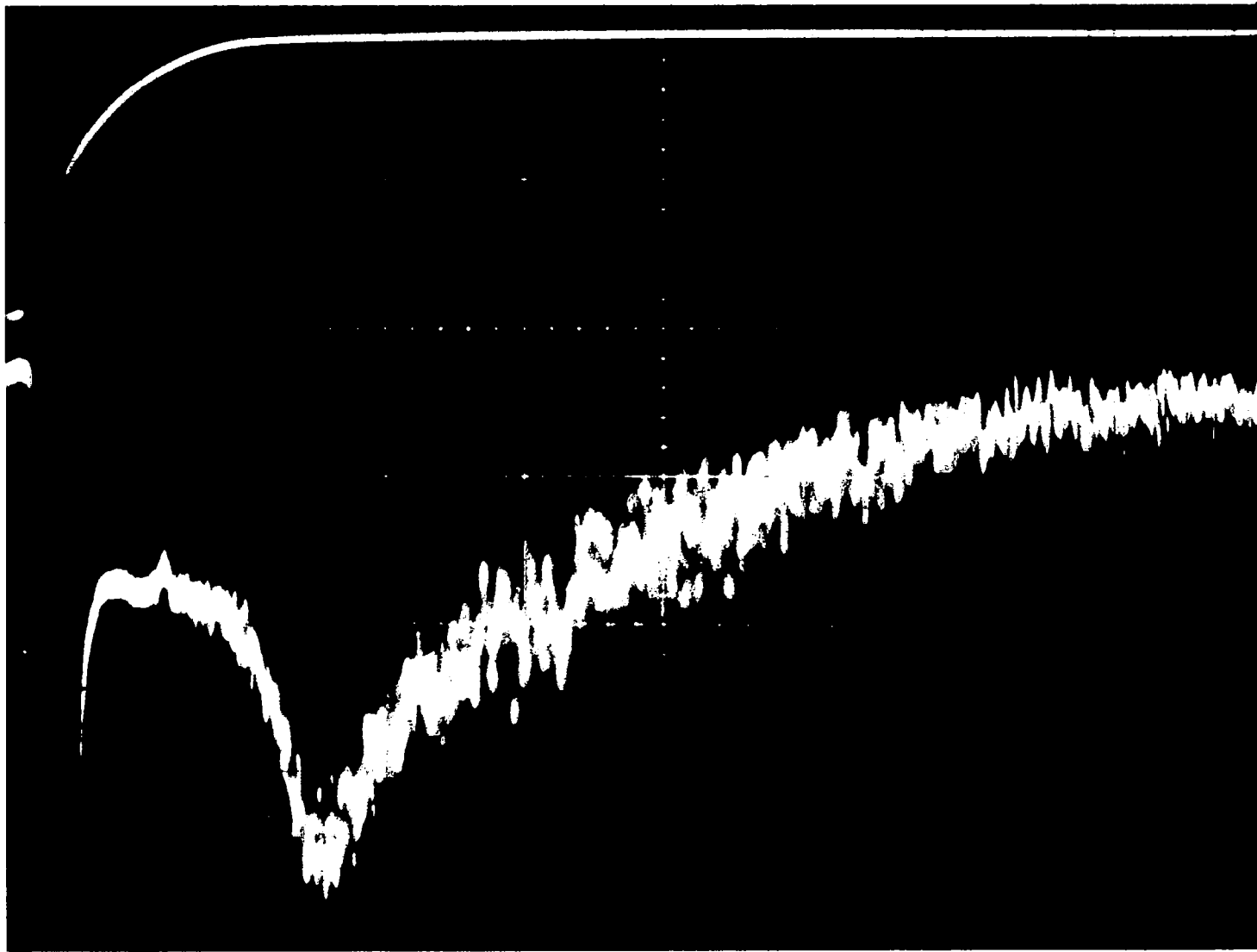
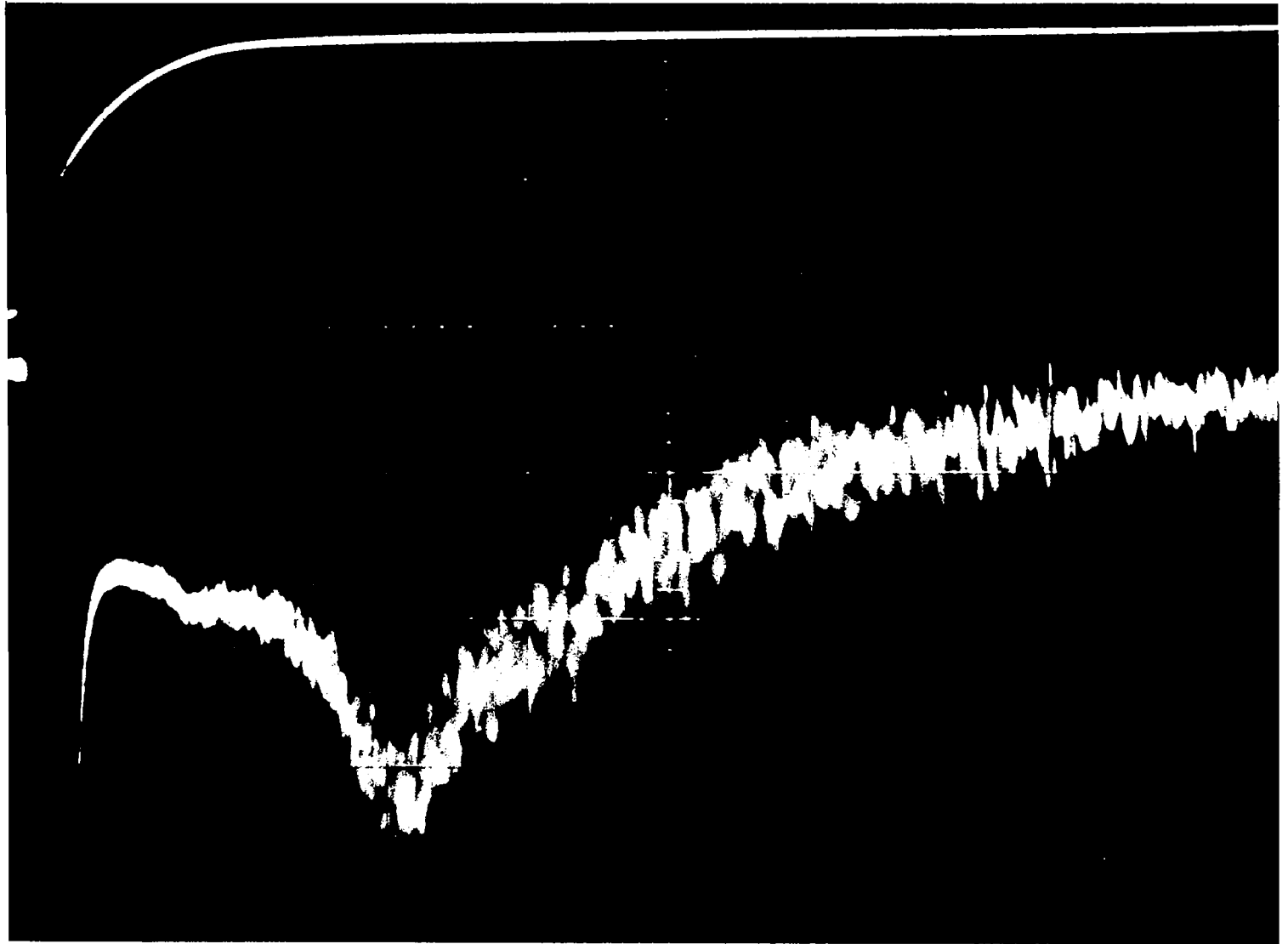3 km   6 km   10μsec/div

Figure 8

31

Figure 9a

3km

6km
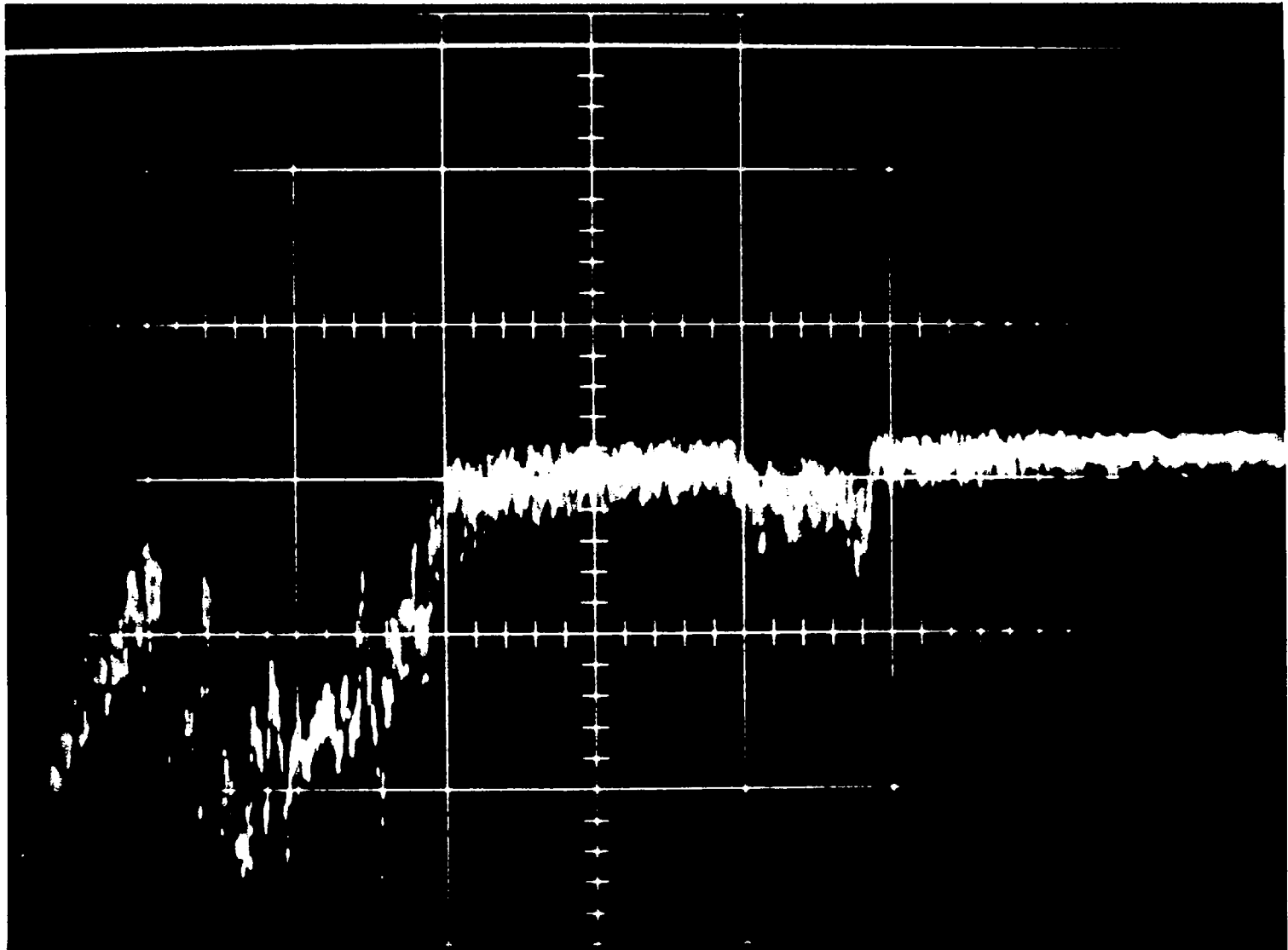
5 μsec/div

3 km   6 km
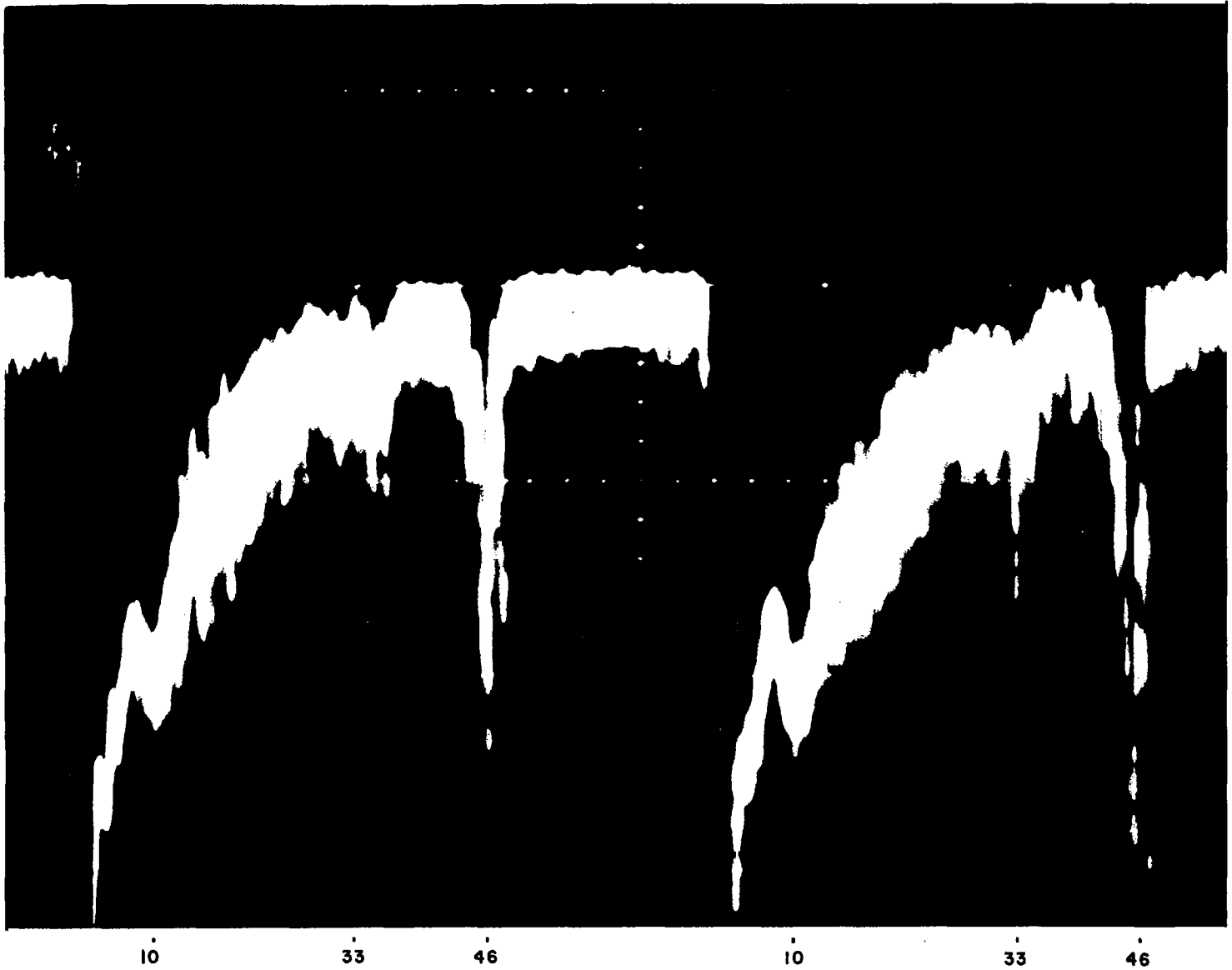
Figure 9b

5μsec/div

33

Figure 10

20 μsec/div

mission shows the same structure and yields comparable values for the return as a function of height (taking the pulse energy into consideration).

The results given here should be regarded as preliminary and are indicative of the promise that optical radar holds for studies of the atmosphere.

REFERENCES

1. E. H. Synge
   A method of investigating the higher atmosphere.
   Phil. Mag. 9, 1014 (1930).

2. M. A. Tuve, et. al.
   A new experimental method for study of the upper atmosphere.
   Terr. Mag. Atmos. Elect. 40, 452 (1935).

3. E. O. Hulbert
   Observations of a searchlight beam to an altitude of 28 km.
   J. Opt. Soc. Amer. 27, 377 (1937).

4. E. A. Johnson, et. al.
   The measurement of light by the upper atmosphere from a searchlight beam.
   J. Opt. Soc. Amer. 29, 512 (1939).

5. L. Elterman
   The measurement of stratospheric density distribution with the search-
   light technique.
   Geosphys. Res. Papers #10 (1951).

6. Bauer and Katzenstein
   State of the earth's atmosphere in Artic.
   Reports 9-14, Univ. of Alaska.

7. L. Elterman
   Seasonal trends of temperature, density, and pressure in the stratosphere
   obtained with the searchlight technique.
   Geophys. Res. Papers #29 (1954).

8. S. Friedland, J. Katzenstein, M. Zatzick
   Pulsed searchlighting the atmosphere.
   J. Geosphys. Res. 61, 415 (1956).

9. G. V. Rosenberg
   Light scattering in the earth's atmosphere.
   Soviet Physics Uspekhi 3, 346 (1960).

10. F. E. Volz, R. M. Goody
    The intensity of the twlight and upper atmospheric dust.
    J. of the Atmos. Sci. 19, 385 (1962).

11. G. Newkirk, Jr., John A. Eddy
    Light scattering by particles in the upper atmosphere.
    J. of the Atmos. Sci. 21, 35 (1964).

12. C. E. Junge, J. E. Manson
    Stratospheric aerosol studies.
    J. of Geophys. Res. 66, 2163 (1961).

13. G. Fiocco, L. D. Smullin
    Detection of scattering layers in the upper atmosphere (60-140 km)
    by optical radar.
    Nature 199, 1275 (1963).

14. G. Fiocco, G. Grams
    Observations of the aerosol layer at 20 km by optical radar.
    J. Atmos. Sci. 21, 323 (1964).

15. R. J. H. Collis, M. G. H. Ligda
    Laser radar echoes from the stratified clear atmosphere.
    Nature 203, 508 (1964).

16. R. J. H. Collis, F. G. Fernald, M. G. H. Ligda
    Laser radar echoes from a stratified clear atmosphere.
    Nature 203, 1274 (1964).

17. G. de Vaucouleurs
    Ann. Phys. 6, 211 (1951).

18. L. Elterman
    Atmospheric attenuation model, 1964, in the ultraviolet, visible, and
    infrared regions for altitudes to 50 km.
    D. D. C. No. AD 607859, A. F. C. R. L., 64-740 (1964).

19. R. H. Giese, E. de Bary, K. Bullrich, C. D. Vinnemann
    Akad. d. dtsch. Wiss., Berlin (1962).

20. K. Bullrich
    Scattered radiation in the atmosphere and the natural aerosol.
    Advances in Geophys. #10, Academic Press, New York, 99 (1964).

21. D. Deirmendjian
    Scattering and polarization properties of polydispersed suspensions with
    partial absorption.
    Electromagnetic scattering, edited by M. Kerker, 171, Macmillan,
    New York (1963)

22. R. Penndorf
    The vertical distribution of Mie particles in the troposphere.
    Geophys, Res. Paper, U. S. A. F. 25.

23. F. Rossler, E. Vassy
    Lumière solarie diffusée par l'atmosphère, measurée à bord d'une fusée
    Veronique; distribution verticale des aérosols, Compt. rend. Acad.
    Sci., Paris 254, 2041.

24. A. Ye. Mikirov
    An investigation into the brightness of the sky and the scatter
    co-efficient of the upper atmosphere.
    Planetary Space Sci. 11, 417 (1963).

25. B. R. Clemesha, G. S. Kent, R. W. H. Wright
    A study of the feasibility of measuring atmospheric densities by
    using a laser-searchlight technique.
    AF-AFOSR, 616 (1965).

26. W. C. Bain, M. C. W. Sandford
    Light scatter from a laser beam at heights above 40 km.
    J. A. T. P. 28, 543 (1966).

27. G. Fiocco, G. Colombo
    Optical radar results and meteoric fragmentation.
    J. of Geophys. Res. 69, 1795 (1964).

28. D. Deirmendjian
    Note on laser detection of atmospheric dust layers.
    J. Geophys. Res. 70, 743 (1965).

29. Shockly and Pierce
    A theory of noise for electron multipliers.
    Proc. I. R. E. (1938).

30. Norden-Ketay
    Correlation of data concerning visible and near infrared radiation
    from the light sky.
    Final report no. 152R0001, Contr. Af 18 (600)-1746 (1957).

31. E. N. Pavlova, S. F. Rodinov, E. D. Sholovkhova
    Energy distribution in the spectrum of the luminosity of the night sky.
    Doklady Ak. Nauk., 98 (1954).

32. D. Deirmendjian, R. J. Clasen
    Light scattering on partially absorbing homogeneous spheres of
    finite size.
    U. S. A. F. Project Rand, R-393-PR, (1962)

Mie Scattering Intensity Functions for Backscatter

The scattered intensity for vertically polarized light incident on a sphere of radius r is given as

$$I = \frac{i}{k^2 z^2} I_o \ ,$$

where

I_o = the intensity of the incident wave

i = the scattered intensity function

$k = \frac{2\pi}{\lambda}$, the free-space propagation constant

λ = the wavelength of the incident light

and z = the distance from scatterer to observer.

The scattered intensity function is given as

$$i = /S/^2 = S*S,$$

where S is given from Mie theory (cf. Deirmendjian[32]).

The value of the intensity function i which is proportional to the intensity of the light backscattered per unit solid angle, for γ = .05(.01)2, 2(.1)50 and η = 1.5, is listed in the following table. An IBM 1620 computer was used for these calculations. The scattering coefficients, a_m and b_m, were terminated when $/a_m/$ and $/b_m/ \leq 10^{-8}$.

TABLE OF INTENSITY FUNCTIONS FOR BACKSCATTTER (η =1.5)

ALPHA	NO. OF TERMS	I
.05	2	.13502860E-08
.06	2	.40301477E-08
.07	3	.10157209E-07
.08	3	.22618487E-07
.09	3	.45822702E-07
.10	3	.86157357E-07
.11	3	.15250345E-06
.12	3	.25680676E-06
.13	3	.41470445E-06
.14	3	.64620508E-06
.15	3	.97642091E-06
.16	3	.14363499E-05
.17	3	.20637079E-05
.18	3	.29038031E-05
.19	3	.40104589E-05
.20	3	.54469735E-05
.21	3	.72871267E-05
.22	3	.96162074E-05
.23	4	.12532092E-04
.24	4	.16146344E-04
.25	4	.20585336E-04
.26	4	.25991400E-04
.27	4	.32524005E-04
.28	4	.40360930E-04
.29	4	.49699473E-04
.30	4	.60757638E-04
.31	4	.73775359E-04
.32	4	.89015691E-04
.33	4	.10676602E-03
.34	4	.12733921E-03
.35	4	.15107486E-03
.36	4	.17834028E-03
.37	4	.20953179E-03
.38	4	.24507570E-03
.39	4	.28542925E-03
.40	4	.33108190E-03
.41	4	.38255586E-03
.42	4	.44040710E-03
.43	4	.50522656E-03
.44	4	.57763994E-03
.45	4	.65830909E-03
.46	4	.74793247E-03
.47	4	.84724503E-03
.48	4	.95701915E-03
.49	4	.10780642E-02
.50	4	.12112274E-02
.51	5	.13573926E-02
.52	5	.15174807E-02
.53	5	.16924494E-02
.54	5	.18832922E-02
.55	5	.20910375E-02
.56	5	.23167475E-02

ALPHA	NO. OF TERMS	I
.57	5	.25615177E-02
.58	5	.28264748E-02
.59	5	.31127748E-02
.60	5	.34216017E-02
.61	5	.37541648E-02
.62	5	.41116968E-02
.63	5	.44954498E-02
.64	5	.49066939E-02
.65	5	.53467125E-02
.66	5	.58167990E-02
.67	5	.63182532E-02
.68	5	.68523766E-02
.69	5	.74204671E-02
.70	5	.80238155E-02
.71	5	.86636985E-02
.72	5	.93413736E-02
.73	5	.10058073E-01
.74	5	.10815000E-01
.75	5	.11613312E-01
.76	5	.12454136E-01
.77	5	.13338521E-01
.78	5	.14267480E-01
.79	5	.15241941E-01
.80	5	.16262760E-01
.81	5	.17330713E-01
.82	5	.18446461E-01
.83	5	.19610579E-01
.84	5	.20823526E-01
.85	5	.22085620E-01
.86	5	.23397068E-01
.87	5	.24757922E-01
.88	6	.26168077E-01
.89	6	.27627266E-01
.90	6	.29135068E-01
.91	6	.30690838E-01
.92	6	.32293776E-01
.93	6	.33942860E-01
.94	6	.35636860E-01
.95	6	.37374332E-01
.96	6	.39153596E-01
.97	6	.40972743E-01
.98	6	.42829588E-01
.99	6	.44721763E-01
1.00	6	.46646578E-01
1.01	6	.48601114E-01
1.02	6	.50582187E-01
1.03	6	.52586342E-01
1.04	6	.54609843E-01
1.05	6	.56648712E-01
1.06	6	.58698690E-01
1.07	6	.60755221E-01
1.08	6	.62813563E-01
1.09	6	.64868641E-01
1.10	6	.66915175E-01
1.11	6	.68947622E-01

ALPHA	NO. OF TERMS	I
1.12	6	.70960231E-01
1.13	6	.72947019E-01
1.14	6	.74901798E-01
1.15	6	.76818217E-01
1.16	6	.78689736E-01
1.17	6	.80509689E-01
1.18	6	.82271238E-01
1.19	6	.83967503E-01
1.20	6	.85591503E-01
1.21	6	.87136221E-01
1.22	6	.88594603E-01
1.23	6	.89959679E-01
1.24	6	.91224430E-01
1.25	6	.92382044E-01
1.26	6	.93425753E-01
1.27	6	.94348999E-01
1.28	6	.95145448E-01
1.29	6	.95809025E-01
1.30	6	.96333908E-01
1.31	6	.96714720E-01
1.32	7	.96946428E-01
1.33	7	.97024482E-01
1.34	7	.96944829E-01
1.35	7	.96704012E-01
1.36	7	.96299156E-01
1.37	7	.95728070E-01
1.38	7	.94989351E-01
1.39	7	.94082343E-01
1.40	7	.93007242E-01
1.41	7	.91765189E-01
1.42	7	.90358253E-01
1.43	7	.88789597E-01
1.44	7	.87063421E-01
1.45	7	.85185085E-01
1.46	7	.83161176E-01
1.47	7	.80999479E-01
1.48	7	.78709132E-01
1.49	7	.76300602E-01
1.50	7	.73785752E-01
1.51	7	.71177864E-01
1.52	7	.68491697E-01
1.53	7	.65743450E-01
1.54	7	.62950872E-01
1.55	7	.60133149E-01
1.56	7	.57311021E-01
1.57	7	.54506660E-01
1.58	7	.51743703E-01
1.59	7	.49047201E-01
1.60	7	.46443497E-01
1.61	7	.43960230E-01
1.62	7	.41626218E-01
1.63	7	.39471271E-01
1.64	7	.37526133E-01
1.65	7	.35822334E-01
1.66	7	.34391914E-01

ALPHA	NO. OF TERMS	I
1.67	7	.33267348E-01
1.68	7	.32481233E-01
1.69	7	.32066110E-01
1.70	7	.32054158E-01
1.71	7	.32476962E-01
1.72	7	.33365220E-01
1.73	7	.34748439E-01
1.74	7	.36654646E-01
1.75	7	.39110049E-01
1.76	7	.42138820E-01
1.77	7	.45762748E-01
1.78	7	.50000909E-01
1.79	7	.54869535E-01
1.80	7	.60381671E-01
1.81	7	.66547024E-01
1.82	8	.73371743E-01
1.83	8	.80858400E-01
1.84	8	.89005804E-01
1.85	8	.97808847E-01
1.86	8	.10725883E+00
1.87	8	.11734319E+00
1.88	8	.12804577E+00
1.89	8	.13934691E+00
1.90	8	.15122367E+00
1.91	8	.16364992E+00
1.92	8	.17659683E+00
1.93	8	.19003289E+00
1.94	8	.20392446E+00
1.95	8	.21823587E+00
1.96	8	.23292989E+00
1.96	8	.23292989E+00
1.97	8	.24796806E+00
1.98	8	.26331090E+00
1.99	8	.27891833E+00
2.00	8	.29474993E+00
2.10	8	.45670752E+00
2.20	8	.60066344E+00
2.30	8	.69661886E+00
2.40	9	.71720048E+00
2.50	9	.64653164E+00
2.60	9	.51468397E+00
2.70	9	.42340074E+00
2.80	9	.49196896E+00
2.90	9	.76350889E+00
3.00	10	.12024007E+01
3.10	10	.17489185E+01
3.20	10	.23268425E+01
3.30	10	.27926815E+01
3.40	10	.29123056E+01
3.50	10	.25534421E+01
3.60	11	.19710983E+01
3.70	11	.16145081E+01
3.80	11	.17487196E+01
3.90	11	.24757479E+01
4.00	11	.38763291E+01
4.10	11	.59065156E+01

ALPHA	NO. OF TERMS	I
4.20	12	.79164068E+01
4.30	12	.85783073E+01
4.40	12	.75030883E+01
4.50	12	.58236767E+01
4.60	12	.46135161E+01
4.70	12	.43852417E+01
4.80	12	.55818754E+01
4.90	13	.88263203E+01
5.00	13	.13774256E+02
5.10	13	.17297874E+02
5.20	13	.17205956E+02
5.30	13	.15128195E+02
5.40	13	.13078473E+02
5.50	13	.12142477E+02
5.60	14	.13090934E+02
5.70	14	.16762583E+02
5.80	14	.22258469E+02
5.90	14	.25349429E+02
6.00	14	.25118504E+02
6.10	14	.23848810E+02
6.20	14	.23457079E+02
6.30	15	.25613627E+02
6.40	15	.32132213E+02
6.50	15	.42704926E+02
6.60	15	.45817357E+02
6.70	15	.37075923E+02
6.80	15	.29067260E+02
6.90	15	.25120175E+02
7.00	16	.25691364E+02
7.10	16	.33489304E+02
7.20	16	.55090779E+02
7.30	16	.90141331E+02
7.40	16	.90661177E+02
7.50	16	.62508313E+02
7.60	16	.38983666E+02
7.70	17	.25278834E+02
7.80	17	.22521615E+02
7.90	17	.33505332E+02
8.00	17	.74093851E+02
8.10	17	.13780711E+03
8.20	17	.12766249E+03
8.30	17	.94845903E+02
8.40	17	.59092571E+02
8.50	18	.34657784E+02
8.60	18	.31306858E+02
8.70	18	.50745064E+02
8.80	18	.11866608E+03
8.90	18	.15205032E+03
9.00	18	.12599865E+03
9.10	18	.10734804E+03
9.20	19	.66746654E+02
9.30	19	.42394478E+02
9.40	19	.53508154E+02
9.50	19	.11102509E+03
9.60	19	.21456061E+03

ALPHA	NO. OF TERMS	I
9.70	19	.13431643E+03
9.80	19	.10977279E+03
9.90	19	.90659299E+02
10.00	20	.42376588E+02
10.10	20	.32191585E+02
10.20	20	.67552649E+02
10.30	20	.21880927E+03
10.40	20	.22397408E+03
10.50	20	.13921510E+03
10.60	20	.12594854E+03
10.70	21	.61581015E+02
10.80	21	.13248550E+02
10.90	21	.23505195E+02
11.00	21	.86074993E+02
11.10	21	.30866752E+03
11.20	21	.15023294E+03
11.30	21	.15738015E+03
11.40	21	.16400932E+03
11.50	22	.30394428E+02
11.60	22	.21231568E+02
11.70	22	.54247465E+02
11.80	22	.21885917E+03
11.90	22	.11579256E+03
12.00	22	.91012872E+02
12.10	22	.15285382E+03
12.20	22	.13794737E+03
12.30	23	.16209953E+02
12.40	23	.46962345E+02
12.50	23	.13390631E+03
12.60	23	.20988002E+03
12.70	23	.56320926E+02
12.80	23	.76212952E+02
12.90	23	.14699098E+03
13.00	23	.22667992E+02
13.10	24	.12540805E+02
13.20	24	.52925238E+02
13.30	24	.41163792E+03
13.40	24	.65575668E+02
13.50	24	.75012132E+02
13.60	24	.11595663E+03
13.70	24	.94856110E+02
13.80	24	.35482524E+01
13.90	25	.17089495E+02
14.00	25	.90498632E+02
14.10	25	.53989723E+02
14.20	25	.39677485E+02
14.30	25	.80492169E+02
14.40	25	.19290860E+03
14.50	25	.10217190E+01
14.60	25	.25973989E+02
14.70	26	.47890618E+02
14.80	26	.80104342E+02
14.90	26	.48137922E+01
15.00	26	.16358531E+02
15.10	26	.68982464E+02

ALPHA	NO. OF TERMS	I
15.20	26	.71771138E+02
15.30	26	.14017559E+02
15.40	26	.30028225E+02
15.50	27	.39587126E+03
15.60	27	.42658130E+01
15.70	27	.96622746E+01
15.80	27	.17343174E+02
15.90	27	.16335753E+03
16.00	27	.76351473E+00
16.10	27	.84364673E+01
16.20	27	.32300730E+02
16.30	28	.15790698E+02
16.40	28	.55238319E+01
16.50	28	.14962026E+02
16.60	28	.47881435E+02
16.70	28	.18240927E+02
16.80	28	.38784182E+01
16.90	28	.27255849E+01
17.00	28	.56487664E+02
17.10	29	.16150537E+02
17.20	29	.48386316E+01
17.30	29	.16740800E+02
17.40	29	.45894860E+02
17.50	29	.16087004E+02
17.60	29	.19705469E+02
17.70	29	.10411957E+03
17.80	29	.33708388E+02
17.90	30	.24157562E+02
18.00	30	.96002197E+01
18.10	30	.29660771E+03
18.20	30	.18652911E+01
18.30	30	.51201140E+02
18.40	30	.72970969E+03
18.50	30	.63079310E+02
18.60	30	.29923285E+02
18.70	31	.16832878E+02
18.80	31	.74800711E+01
18.90	31	.15070950E+02
19.00	31	.83167369E+01
19.10	31	.12339733E+03
19.20	31	.22558680E+03
19.30	31	.14181306E+03
19.40	31	.56427725E+02
19.50	32	.65559994E+02
19.60	32	.14143381E+02
19.70	32	.39511699E+00
19.80	32	.44426891E+02
19.90	32	.24419204E+03
20.00	32	.29961587E+03
20.10	32	.23375773E+03
20.20	32	.11596857E+03
20.30	32	.51086411E+02
20.40	33	.77783993E+01
20.50	33	.39435190E+02
20.60	33	.20708992E+03

ALPHA	NO. OF TERMS	I
20.70	33	.31472683E+03
20.80	33	.29988998E+03
20.90	33	.24928963E+03
21.00	33	.50042130E+03
21.10	33	.59572135E+02
21.20	34	.31724385E+02
21.30	34	.13505764E+03
21.40	34	.56071263E+03
21.50	34	.41517654E+03
21.60	34	.31664792E+03
21.70	34	.21105834E+03
21.80	34	.83135332E+02
21.90	34	.37421848E+02
22.00	35	.34624408E+02
22.10	35	.38928791E+03
22.20	35	.71075433E+03
22.30	35	.58799865E+03
22.40	35	.45489568E+03
22.50	35	.12788653E+03
22.60	35	.33418703E+02
22.70	35	.25035181E+02
22.80	35	.68105555E+02
22.90	36	.71872929E+03
23.00	36	.60788941E+03
23.10	36	.74105903E+03
23.20	36	.48540975E+03
23.30	36	.14733266E+03
23.40	36	.94460027E+02
23.50	36	.60489955E+02
23.60	36	.50021652E+03
23.70	37	.55324687E+03
23.80	37	.48993209E+03
23.90	37	.70769978E+03
24.00	37	.34508996E+03
24.10	37	.15484995E+03
24.20	37	.12589473E+03
24.30	37	.16681242E+03
24.40	37	.11042650E+04
24.50	37	.50929140E+03
24.60	38	.55436618E+03
24.70	38	.56456620E+03
24.80	38	.12793942E+03
24.90	38	.10995013E+03
25.00	38	.97565380E+02
25.10	38	.64129920E+03
25.20	38	.71510744E+03
25.30	38	.57896730E+03
25.40	39	.97986898E+03
25.50	39	.26307044E+03
25.60	39	.10422710E+03
25.70	39	.98209016E+02
25.80	39	.84224308E+02
25.90	39	.85839036E+03
26.00	39	.41076072E+03
26.10	39	.65722298E+03

ALPHA	NO. OF TERMS	I
26.20	39	.11643437E+04
26.30	40	.21514097E+03
26.40	40	.26356532E+03
26.50	40	.18736771E+03
26.60	40	.11766814E+04
26.70	40	.31008069E+03
26.80	40	.30183229E+03
26.90	40	.80957045E+03
27.00	40	.32909977E+03
27.10	41	.26796353E+03
27.20	41	.37816278E+03
27.30	41	.27238377E+03
27.40	41	.95838445E+03
27.50	41	.35752008E+03
27.60	41	.45174177E+03
27.70	41	.10423826E+04
27.80	41	.10113998E+03
27.90	41	.28992273E+03
28.00	42	.29300431E+03
28.10	42	.18024424E+04
28.20	42	.46998204E+03
28.30	42	.45115214E+03
28.40	42	.97440752E+03
28.50	42	.13080587E+03
28.60	42	.32351656E+03
28.70	42	.38569725E+03
28.80	43	.22539190E+03
28.90	43	.39775070E+03
29.00	43	.27857527E+03
29.10	43	.43848120E+03
29.20	43	.12002333E+04
29.30	43	.31616737E+03
29.40	43	.73103526E+03
29.50	43	.52928538E+03
29.60	43	.66141408E+03
29.70	44	.21045325E+03
29.80	44	.19079271E+03
29.90	44	.66274303E+03
30.00	44	.97042389E+02
30.10	44	.48134430E+03
30.20	44	.92703663E+03
30.30	44	.32562261E+04
30.40	44	.46045826E+03
30.50	45	.27089253E+03
30.60	45	.36912540E+03
30.70	45	.85464601E+02
30.80	45	.22141586E+03
30.90	45	.70473577E+03
31.00	45	.66682203E+03
31.10	45	.71004655E+03
31.20	45	.34466540E+03
31.30	45	.32982308E+03
31.40	46	.13420407E+04
31.50	46	.25705065E+03
31.60	46	.68426681E+03

ALPHA	NO. OF TERMS	I
31.70	46	.10583144E+04
31.80	46	.85128571E+03
31.90	46	.32095278E+03
32.00	46	.14840836E+03
32.10	46	.31189896E+03
32.20	47	.12924743E+03
32.30	47	.45625785E+03
32.40	47	.13863371E+04
32.50	47	.32693316E+04
32.60	47	.58370811E+03
32.70	47	.13564858E+03
32.80	47	.88448309E+02
32.90	47	.13727063E+03
33.00	47	.15062819E+03
33.10	48	.56453732E+03
33.20	48	.17379457E+04
33.30	48	.12225815E+04
33.40	48	.54226768E+03
33.50	48	.12445739E+03
33.60	48	.40638663E+03
33.70	48	.17003675E+03
33.80	48	.31002897E+03
33.90	48	.10887299E+04
34.00	49	.13088577E+04
34.10	49	.85240229E+03
34.20	49	.36075199E+03
34.30	49	.13249310E+03
34.40	49	.15660085E+03
34.50	49	.36171448E+03
34.60	49	.74481631E+03
34.70	49	.18357457E+04
34.80	50	.71669091E+03
34.90	50	.49718401E+03
35.00	50	.91897598E+02
35.10	50	.10193976E+02
35.20	50	.16769924E+03
35.30	50	.35699423E+03
35.40	50	.19624538E+04
35.50	50	.12901977E+04
35.60	50	.66465514E+03
35.70	51	.26767966E+03
35.80	51	.15923546E+02
35.90	51	.67977252E+02
36.00	51	.11225315E+03
36.10	51	.33583784E+03
36.20	51	.20436402E+04
36.30	51	.79948182E+03
36.40	51	.79260618E+03
36.50	52	.10187172E+03
36.60	52	.94797110E+02
36.70	52	.20117859E+03
36.80	52	.20170737E+03
36.90	52	.79087922E+03
37.00	52	.60450420E+03
37.10	52	.46263217E+03

ALPHA	NO. OF TERMS	I
37.20	52	.80657525E+03
37.30	52	.33265546E+02
37.40	53	.13515200E+03
37.50	53	.22485501E+03
37.60	53	.30511451E+03
37.70	53	.15234001E+04
37.80	53	.18098063E+03
37.90	53	.32369719E+03
38.00	53	.13174137E+04
38.10	53	.23536015E+02
38.20	54	.75206393E+02
38.30	54	.99249123E+03
38.40	54	.76162530E+03
38.50	54	.33859893E+03
38.60	54	.23859457E+03
38.70	54	.55685281E+03
38.80	54	.19763446E+03
38.90	54	.67696935E+02
39.00	55	.17512245E+02
39.10	55	.10496304E+02
39.20	55	.99018557E+03
39.30	55	.14088068E+03
39.40	55	.36618878E+03
39.50	55	.64853179E+03
39.60	55	.83918340E+02
39.70	55	.10064538E+03
39.80	55	.13354987E+01
39.90	56	.41342935E+03
40.00	56	.91319859E+02
40.10	56	.35084801E+02
40.20	56	.54888891E+03
40.30	56	.17995580E+03
40.40	56	.50312551E+02
40.50	56	.12927818E+03
40.60	56	.18365916E+01
40.70	57	.23828335E+03
40.80	57	.15157622E+02
40.90	57	.42520502E+01
41.00	57	.14145119E+04
41.10	57	.67958641E+02
41.20	57	.84548532E+02
41.30	57	.26016635E+03
41.40	57	.72412873E+03
41.50	58	.91666641E+02
41.60	58	.28504703E+01
41.70	58	.21001575E+03
41.80	58	.29380068E+03
41.90	58	.53975260E+02
42.00	58	.21030572E+03
42.10	58	.30561548E+03
42.20	58	.76846005E+03
42.30	59	.15683816E+03
42.40	59	.36094554E+02
42.50	59	.13654653E+04
42.60	59	.19844692E+02

ALPHA	NO. OF TERMS	I
42.70	59	.12656770E+03
42.80	59	.39430416E+03
42.90	59	.17939564E+04
43.00	59	.65967890E+03
43.10	59	.20521977E+03
43.20	60	.24675639E+03
43.30	60	.16558818E+03
43.40	60	.42184121E+02
43.50	60	.76271658E+03
43.60	60	.37452926E+03
43.70	60	.86340594E+03
43.80	60	.41565553E+03
43.90	61	.88040792E+02
44.00	61	.12636466E+04
44.10	61	.10627308E+03
44.20	61	.22146304E+03
44.30	61	.15433053E+04
44.40	61	.21609190E+04
44.50	61	.83263478E+03
44.60	61	.16680044E+03
44.70	62	.18767295E+03
44.80	62	.13706050E+03
44.90	62	.66417758E+01
45.00	62	.84262011E+03
45.10	62	.42131900E+04
45.20	62	.22981050E+04
45.30	62	.96623802E+03
45.40	62	.17419325E+03
45.50	63	.26631444E+03
45.60	63	.34688827E+02
45.70	63	.20941803E+03
45.80	63	.14881501E+04
45.90	63	.22406225E+04
46.00	63	.20272525E+04
46.10	63	.80386039E+03
46.20	63	.24539672E+04
46.30	64	.32393590E+03
46.40	64	.15387912E+03
46.50	64	.16964161E+04
46.60	64	.26211096E+04
46.70	64	.20939323E+04
46.80	64	.12229490E+04
46.90	64	.28661979E+03
47.00	65	.39589670E+03
47.10	65	.36614503E+03
47.20	65	.21376831E+03
47.30	65	.26933250E+04
47.40	65	.27973767E+04
47.50	65	.25261072E+04
47.60	65	.56778519E+03
47.70	65	.39876068E+03
47.80	66	.23189181E+03
47.90	66	.15378680E+03
48.00	66	.12513857E+04
48.10	66	.26604480E+04

ALPHA	NO. OF TERMS	I
48.20	66	.32591440E+04
48.30	66	.24037596E+04
48.40	64	.56009979E+03
48.50	64	.43457770E+03
48.60	64	.44207736E+03
48.70	64	.15375385E+03
48.80	64	.27969538E+04
48.90	65	.17927601E+04
49.00	65	.33942426E+04
49.10	65	.12844596E+04
49.20	65	.57556912E+03
49.30	65	.98560042E+03
49.40	65	.71462972E+03
49.50	65	.42410267E+04
49.60	65	.19589380E+04
49.70	66	.20591544E+04
49.80	66	.24199168E+04
49.90	66	.64625798E+03
50.00	66	.50265475E+03